
Article:
Xia, W., Liu, Y., Wang, G. et al. (6 more authors) (2020) Frequency and temperature independent (Nb0.5Ga0.5)x(Ti0.9Zr0.1)1-xO2 ceramics with giant dielectric permittivity and low loss. Ceramics International, 46 (3). pp. 2954-2959. ISSN 0272-8842

https://doi.org/10.1016/j.ceramint.2019.09.292

Frequency and temperature independent $(Nb_{0.5}Ga_{0.5})_x(Ti_{0.9}Zr_{0.1})_{1-x}O_2$ ceramics with giant dielectric permittivity and low loss

Weimin Xia [a#], Yiming Liu[a#], Ge Wang [b#], Jinglei Li[c#], Congjun Cao[a], Qingyuan Hu[c], Yuanqing Chen[d], Zhilun Lu [b], Dawei Wang [b*]

a. Faculty of Printing, Packaging, and Digital Media Technology, Xi'an University of Technology, Xi'an 710048, Shaanxi, China.

b. Department of Materials Science and Engineering, University of Sheffield, Sheffield S1 3JD, UK

c. Electronic Materials Research Laboratory, Key Laboratory of the Ministry of Education and International Center for Dielectric Research, Xi'an Jiaotong University, Xi'an 710049, Shaanxi, China.

d. School of Materials Science and Engineering, Xi'an University of Technology, Xi'an 710048, Shaanxi, China.

[#]Author Contributions: Weimin Xia, Yiming Liu, Ge Wang and Jinglei Li contributed equally to this work.

Abstract: Nb^{5+} and Ga^{3+} co-doped $Ti_{0.9}Zr_{0.1}O_2$ ceramics were synthesized using the conventional solid-state reaction method. Single rutile-liked phase of octahedron structure were identified for all compositions in $(Nb_{0.5}Ga_{0.5})_x(Ti_{0.9}Zr_{0.1})_{1-x}O_2$ (NGT) with x = 0.01 to 0.10 by X-ray diffraction patterns coupled with Rietvele refinement. Microstructural scanning image, together with energy dispersive x-ray spectroscopy (EDX), revealed good chemical homogeneity in NGT samples. A giant dielectric permittivity of 5×10^4 and a low loss of 0.02 were obtained in NGT with x=0.01 due to the contribution of electron-pinned and defect-dipole effect. Furthermore, a temperature (-20~120 ^{o}C), frequency (0.1~10^4 Hz) and bias electric field (100~200 V/mm) independent dielectric permittivity and loss are found in this composition, which is critical for potential applications of supercapacitors.

Keywords: Giant dielectric permittivity; frequency-independent; DC bias

*Corresponding to dawei.wang@sheffield.ac.uk

1 Introduction

Over the past few years, a giant permittivity ($\varepsilon' > 10^4$) were reported TiO_2-based ceramics, which have drawn considerable attention for electronic and electrical energy storage devices.[1-3] For example, Nb-doped TiO_2 was reported to exhibit giant dielectric permittivity due to the reduction of Ti^{4+} to Ti^{3+}.[4] For Nb+In co-doped TiO_2, excellent dielectric properties with desirable temperature stability was obtained by means of local oxygen-vacancy trap of the delocalized activation electrons [10-14] Rare earth (RE) elements are also commonly found to optimize dielectric properties, such as Li-doped NiO,[6] La-doped $Sr_{1/8}NiO_4$,[7] etc. [4,8-9]

Recently, increasing number of RE doped TiO_2 has been reported to exhibit giant dielectric permittivity and low loss. In these elements, a combination of A^{3+} andB^{5+} is commonly reported, where A is an acceptor dopant, including In, Ga, Yb, La, Sc, Al, Bi, Er, Sm, Y, etc., and B is a donor dopant, such as Nb, Sb, Ta, and etc. [6,9,13,15-19] It is proposed that giant dielectric permittivity response of these materials is attributed by the generation of the electron-pinned defect-dipole (EPDD). Nevertheless, many controversial statements believed the classical Maxwell induces giant dielectric permittivity–Wagner polarization, including the traditional electrode effects,[14] internal barrier layer capacitor (IBLC) effects, surface barrier layer effects,[20] hopping ions conductivity,[21] and special polaronic relaxation or microscopic inhomogeneities.[12-13]

To understand the origin of giant dielectric permittivity in depth, it was found that EPDD mechanism applied at low temperature while Maxwell-Wagner polarization mechanism is more suitable to hot circumstance. Therefore, to obtain excellent TiO_2-based ceramics with temperature-independent giant dielectric permittivity, an effective way is controlling EPDD's effects while depressing the Maxwell–Wagner interfacial polarization. Actually, many researchers have introduced using La, Zr, etc.[22-24] to form a second phase to modify the dielectric response of $CaCu_3Ti_4O_{12}$ (CCTO) series materials.[25-26] to reduce the effect of Maxwell–Wagner polarization on the giant dielectric

permittivity materials. The grain size reduced and resistance of grain boundary enhanced for La, Zr co-doped CCTO, leading to a stable dielectric permittivity on a high DC bias.[14,21,27–30]. More importantly, it has confirmed that secondary phases of La, Zr, etc. can be diffused into rutile TiO_2 ceramics due to the generation of noncovalent substitution.[31-33] Similar studied was reported for Nb,Ta co-doped TiO_2.

Therefore, a series of $(Nb_{0.5}Ga_{0.5})_x(Ti_{0.9}Zr_{0.1})_{1-x}O_2$ (NGT) ceramics with x=0.00-0.10 were synthesized using traditional solid-state method to examine different dopants on dielectric properties. Ga^{3+} and Nb^{5+} were added into TiO_2 to facilitate the formation of the oxygen-vacancy trap. The crystal structure of NGT ceramics were examined under x-ray diffraction (XRD). The dielectric properties, including dielectric permittivity, loss, temperature stabilities, frequency stabilities, and DC bias stability depending was investigated. As a result, the giant dielectric permittivity and depressed dielectric loss were obtained from Ga/Nb co-doped TiO_2 materials due to combined effect of oxygen-vacancy trap and EPDD.

2 Experimental section

2.1 Preparation of NGT ceramics

$(Nb_{0.5}Ga_{0.5})_x(Ti_{0.9}Zr_{0.1})_{1-x}O_2$ ceramics with x=0.00-0.10 were prepared by traditional solid-state reaction method with ZrO_2 (99.99%), rutile TiO_2 (99.98%), Nb_2O_5 (99.98%) and Ga_2O_3 (99.5%) powder as raw material. The samples were sintered from 1350 to 1450 ºC with variation dwelling time in the air to obtain highly density. The compositions with x=0, 0.01, 0.03, 0.05, 0.07, 0.09, and 0.10 were marked as NGT, NGT-1, NGT-3, NGT-5, NGT-7, NGT-9, and NGT-10, respectively.

2.2 Characterization

The crystal structure of NGT ceramics was examined by XRD (D/MAX 2400, Japanese) at a scan step of 0.05º. The microstructural morphology of the ceramics was prepared by grinding, polishing

and thermal etching, followed by examination under SEM (Quanta F250, Germany) with energy dispersive x-ray spectroscopy (EDX) detector. The valent state of NGT ceramics were investigated using X-ray photoelectron spectroscopy (XPS, AXIS ultra DLD, England). Specimens for dielectric measurement were painted silver paste first as electrode, followed by a firing procedure at 500 ºC for 0.5 h. The temperature-dependent and frequency-dependent dielectric properties were measured in the frequency range of 0.1~1 MHz and temperature range of -20~120 ºC, respectively, using a broadband dielectric spectrometer (Novocontrol alpha-A, German).

3 Results and Discussion

3.1 The phase microstructure

The XRD patterns of NGT ceramics with x=0.00-0.10 are given in Fig.1 (a), exhibiting a single rutile phase for all ceramics (PDF: 04-005-4859).[1,15,36] The intensity of (211) diffraction peak of NGT ceramics increases with the increase of Nb, Ga content, suggesting that the doping of Nb, Ga may minimize the grain size of ceramics[8] and improve the pinning effects from Nb and Ga atoms.

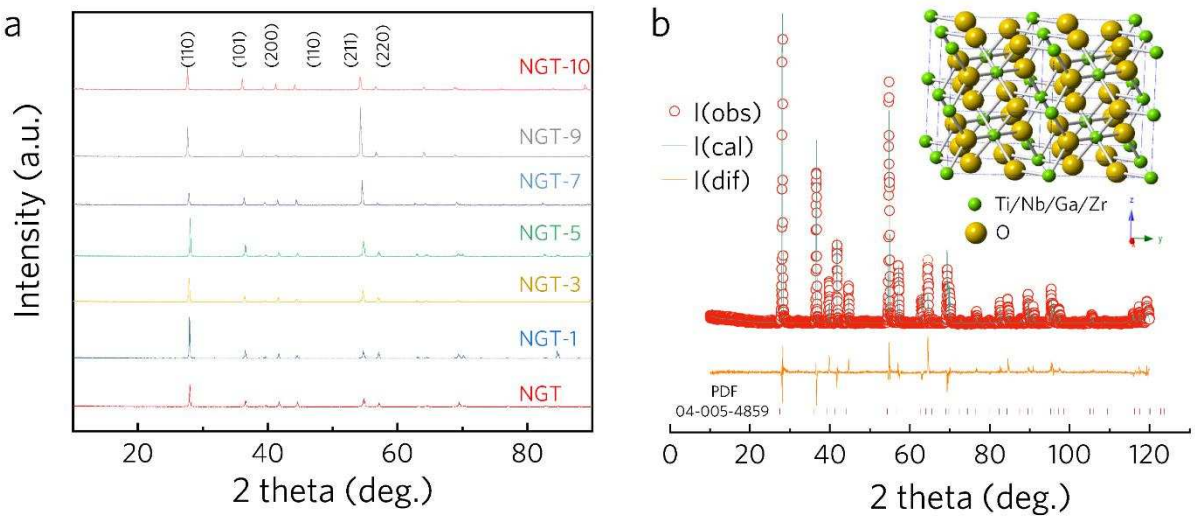

Fig.1. (a) XRD patterns for different NGT ceramics, (b) Rietveld refinement of XRD patterns for NGT-5 based on the tetragonal rutile crystal structure using $P4_2/mmm$. The schematic crystal structure of NGT-5 is given in the inset of Fig.1 (b).

Full pattern Rietveld refinement was performed for Nb, Ga co-doped $Ti_{0.9}Zr_{0.1}O_2$ ceramics, as illustrated in Fig. 1b, with the best fitting factors of R_p=8.3%, R_{wp}=9.1% and χ^2=1.8 being obtained using $P4_2/mmm$. For tetragonal rutile phase, the center site is occupied by a Ti^{4+} or Zr^{4+} ion with radius of 0.745 Å or 0.86 Å, respectively, which is connected with six close O^{2-} ions (radius 1.28 Å), forming [TiO_6] octahedron (Fig.1b). It is worthy noted that Ga^{3+} and Nb^{5+} ions could substitute the place of Ti^{4+} to form [GaO_6 and NbO_6] octahedron, where their radius is 0.62 Å (Ga^{3+}) and 0.78 (Nb^{5+}) 0.78 Å, respectively. Therefore, all samples are obtained as single rutile phase structure, indicating that the dielectric response is not manipulated by the crystal structure.[24,37]

3.2 Microstructural morphology

The microstructure morphology of NGT ceramics were shown in Fig.2 (a-f). The cross-section images of all ceramics appear to be dense, yielding a density of approximately 4.3 g cm^{-3}. The grain size of NGT ceramics reduces significantly from 100 to 40 μm as increasing x concentration from 0.01 to 0.1 due to pinning effect. The EDX element mapping of NGT-10 is illustrated in Fig.3, indicating homogeneous distribution of O, Zr, Nb, Ti and Ga elements.

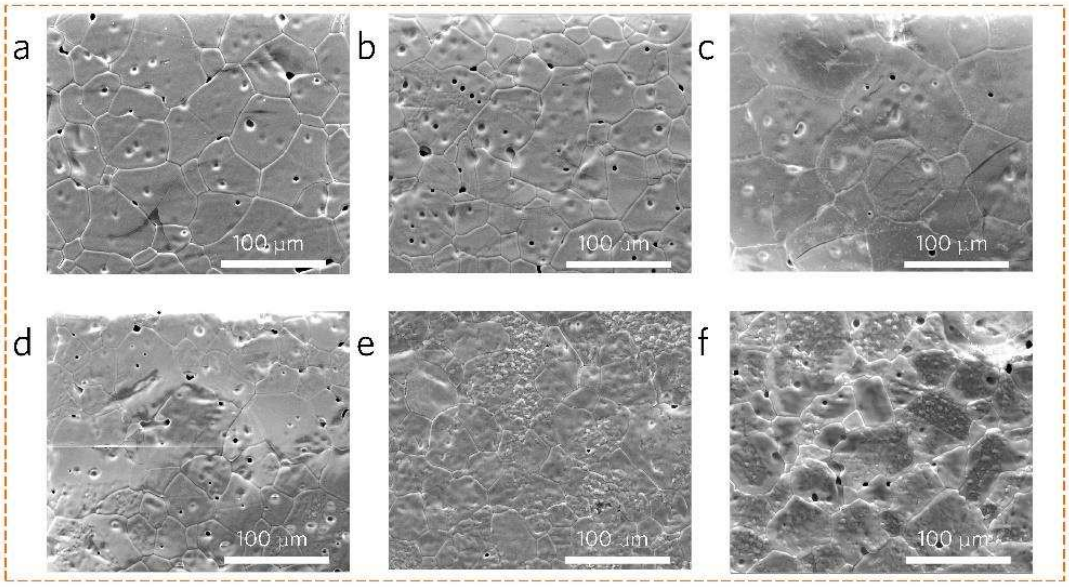

Fig.2. SEM images of $(Ga_{0.5}Nb_{0.5})_x(Ti_{0.9}Zr_{0.1})_{1-x}O_2$ ceramics with (a)x=0.01, (b)x=0.03, (c)x=0.05, (d)x=0.07, (e)x=0.09 and (f)x=0.10.

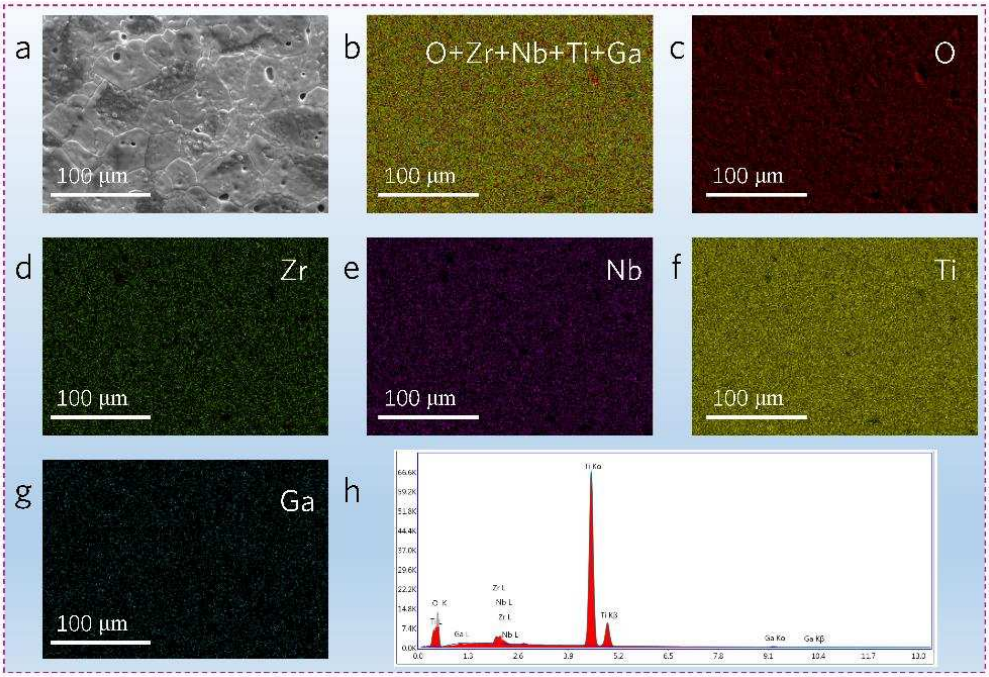

Fig.3. (a) SEM and (b-f) surface EDX element mapping and (h) EDS of $(Ga_{0.5}Nb_{0.5})_x(Ti_{0.9}Zr_{0.1})_{1-x}O_2$ ceramics with x=0.10.

3.3 Valence state analysis

The valence state of elements has a significant influence on the TiO_2-based dielectric materials. Therefore, XPS spectra were performed on NGT-5 to illustrate the valence state of Zr, Nb, O, and Ti ions, as shown in Fig.4. The XPS fitting was performed on Casa. As illustrated in Fig. 4(a), the binding energies of Zr^{4+} $3d_{5/2}$ electronic orbit and $3d_{3/2}$ electronic orbit are 181.87 and 184.27 eV, respectively, which refers to quadrivalent Zr ions.[16] Four Ti binding energy peaks of 464.27, 461.47, 458.67, and 456.97 eV, are considered to be Ti^{4+} $2p_{1/2}$, Ti^{3+} $2p_{1/2}$, $Ti^{3+}2p_{3/2}$, and Ti^{4+} $2p_{3/2}$ electronic orbits, respectively, as shown in Fig. 4(b). The binding energy of $3d_{5/2}$-$3d_{3/2}$ of Nb^{5+} ions is expected to be 207.67-210.67 eV, as shown in Fig. 4(c). Meanwhile, there is no extra Nb 3d from XPS results, indicating pentavalent Nb ions in NGT-5.[27] Besides, as shown in Fig.4 (d), a low binding energy peak of 530.07 eV (shorthand for O_L) and a high one of 531.27 eV (shorthand for O_H) are obtained, which are induced by the negative bivalent oxygen atoms into the Ti-O bond and oxygen vacancy $V\ddot{o}$, respectively. To

balance the charges of the oxygen vacancy $V\ddot{o}$, Ti^{4+} ions intend to reduce to Ti^{3+} in NGT, as shown in Fig.4 (b). The introduction of oxygen vacancies and the reduction of Ti ions are illustrated in equation 1. The introduction of oxygen vacancies trapped with the corresponding complex defect dipoles may affect the dielectric performance of NGT materials.

$$2\mathrm{Ti}O_2 \rightarrow 2Ti' + V\ddot{o} + 3O_o + 1/2O_2 \uparrow \tag{1}$$

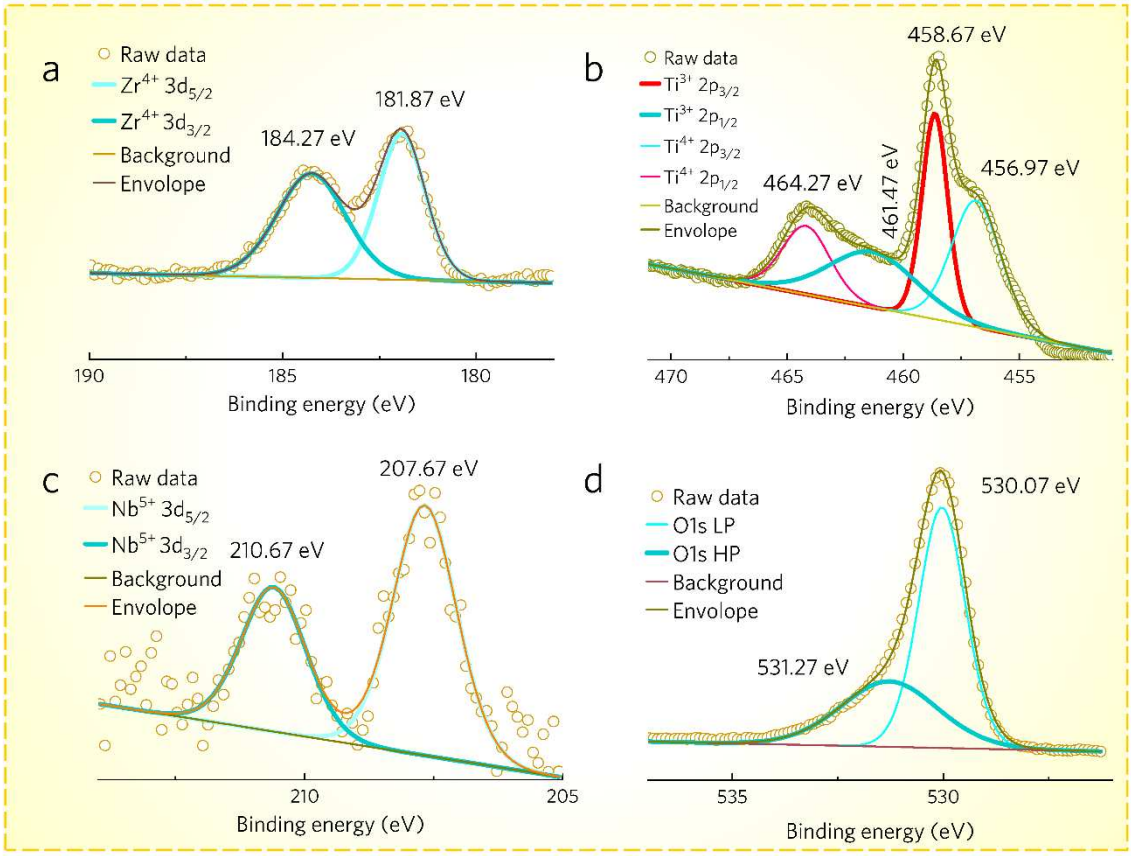

Fig. 4. The XPS results for co-doped NGT-5 ceramics. (a) Zr , (b) Ti, (c) Nb, and (d) O ions.

3.4 Dielectric characterization

The dielectric properties of NGT ceramics were evaluated in a frequency range from 0.1 to 1 kHz, as shown in Fig.5. The frequency-dependent dielectric characterization of NGT-1~10 shows a good frequency stability at low frequency (<200 Hz), indicating that the giant dielectric permittivity of NGT could not be attributed to the interface polarization effect, such as surface

layer effect and Maxwell-Wagner effect. The highest frequency-independent permittivity ~ 7×10^4 is obtained for NGT-1 due to possible weakly-localized electrons in defect-dipole clusters of Nb and Ga. Based on the electron-pinned and defect-dipole theory proposed by the Hu et. al.,[4,34,39] oxygen vacancy is localized by designated lattice defect states to trap the weekly-localized electrons, leading to defect-dipole polarization. Another attracted point observed in NGT-5 is the lower dielectric loss ~ 0.02, exhibiting a frequency-independent character above 10^4 dielectric permittivity. It is worthy noted that the NGT-10 has a maximum dielectric loss, which may be associated with the little reduction of Ga_2O_3 oxides to Ga metal with significantly decreasing oxygen partial pressure under high temperature. The evaporation of Ga ions will enhance the conductivity of samples, leading to the increase of dielectric loss.

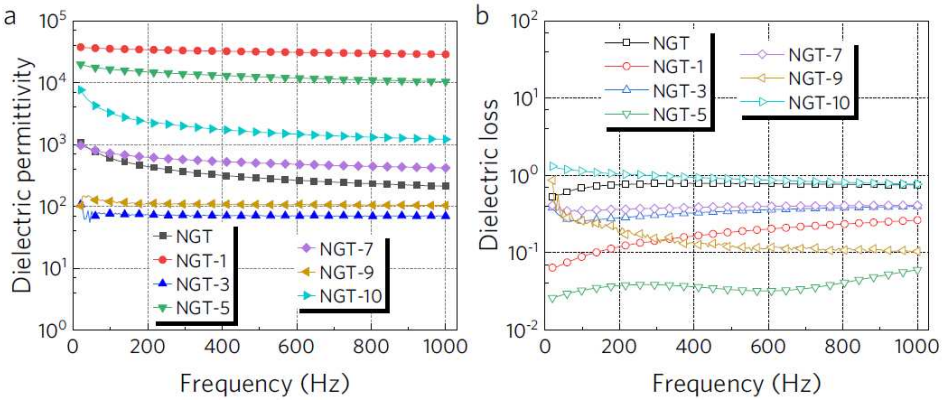

Fig.5 Dielectric permittivity (a) and loss (b) spectrum for various NGT ceramics vs frequency range from 0.1 to 1 kHz.

The temperature- and frequency-dependent dielectric performance of NGT5 ceramics are illustrated in Fig.6. The dielectric permittivity is found to decrease with decreasing temperature and/or frequency in the whole temperature and frequency region. Furthermore, a sharp drop on the dielectric permittivity is observed at a frequency ~ 10 kHz for NGT5 ceramics. Meanwhile, the dielectric loss exhibits a decrease with increasing frequency, as shown in Fig.6 (b). The dielectric behaviour in NGT5 sample at low frequency above 80 °C is considered to be the typical characteristic of Maxwell-Wagner effect, as shown in Fig.6 (c). Additionally, the

dielectric permittivity of NGT5 increases significantly with increases temperature in a frequency range of 0.01 to 100 kHz, further confirming the interface-polarization mechanism due to Nb and Ga co-doping. The temperature-dependent dielectric behaviour in a frequency range from 0.1 to 10MHz is displayed in Fig. 6(d). It is found that the temperature-independent dielectric permittivity of NGT5 decreases with increasing frequency. Compared to the dielectric loss at low frequencies of 0.1, 1, 10 and 100 Hz, the dielectric loss in high frequencies (1 k to 10 MHz) shows relative frequency stability because interface-polarization probably is no longer catching the step of the frequency of the polarizing electric field.

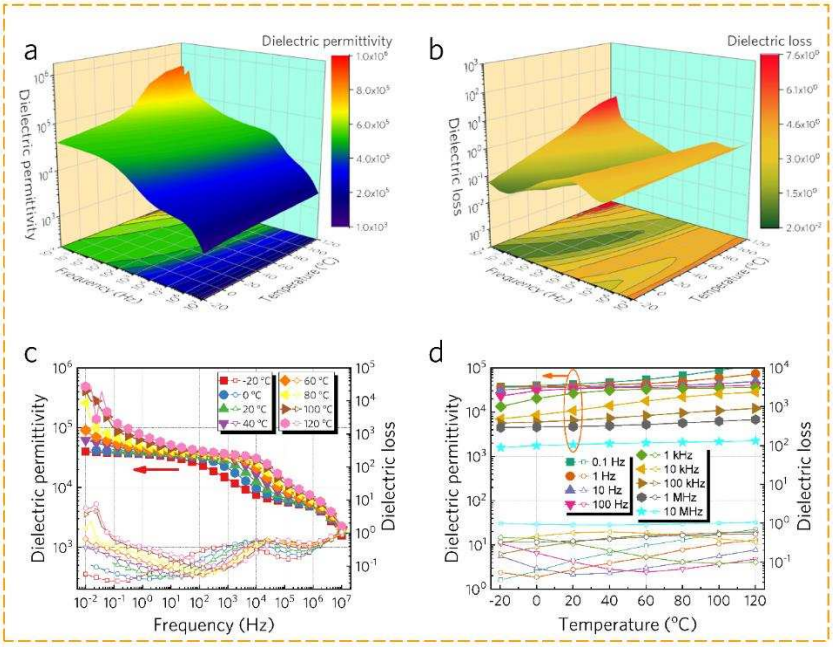

Fig.6 3D view frequency-dependent (a) dielectric permittivity and (b)loss at selected temperature for NGT 5; (c) Frequency-dependent permittivity and loss at selected temperatures for NGT5; (d) Temperature-dependent permittivity and loss at selected frequencies for NGT5.

The frequency-dependent (from 1 to 10 kHz) dielectric properties for NGT5 under various DC bias electric fields are shown in Fig.7.The dielectric permittivity of NGT5 exhibits no obvious change under various bias electric fields from 100 to 200V/mm. However, the dielectric loss of NGT5 changes slightly under various bias electric fields. As reported in the

literatures, [12-14, 20-21] the polarization at ultra-low frequency range (<10 Hz) is mainly dominated by Maxwell-Wagner polarization between samples and electrodes, i.e., the surface barrier layer capacitor effects.[21,40] The existence of interface-polarization in the NGT5 is confirmed in Figs. 5 and 6. Therefore, the various of dielectric loss in the ultra-low frequency region is anticipated to be the traditional Maxwell-Wagner effects. During the application of the external electric field to the samples, the weekly-delocalized electrons are forced or trapped to the oxygen vacancy so that the dielectric loss declines.

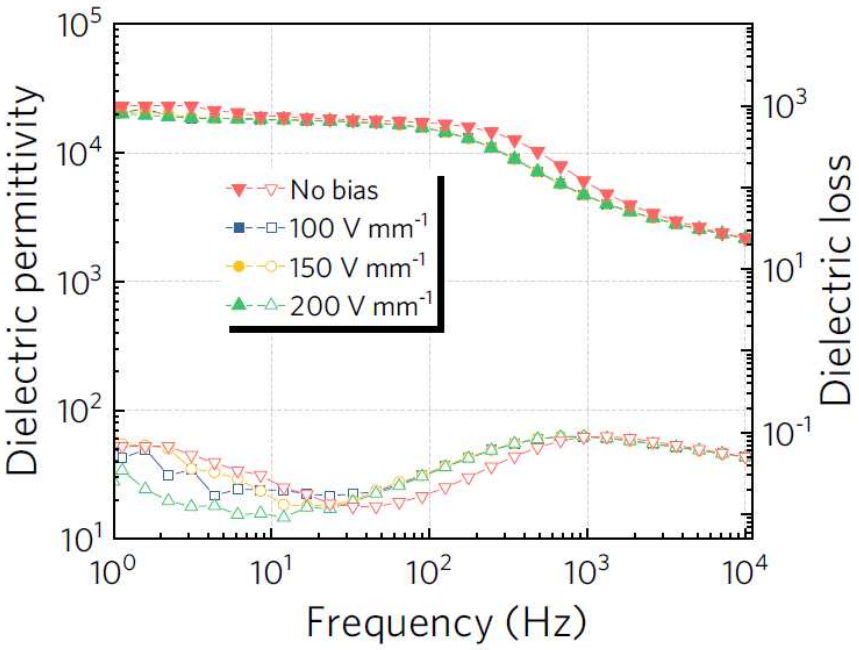

Fig.7. The frequency-dependent dielectric permittivity and loss for NGT-5 under different bias electric fields.

4 Conclusion

In this study, $(Nb_{0.5}Ga_{0.5})_x(Ti_{0.9}Zr_{0.1})_{1-x}O_2$ (NGT, x=0.01~0.10) ceramics were synthesized using a conventional solid-state method. XRD patterns, coupled with Rietveld refinement, prove that all the NGT ceramics possess a rutile-liked octahedron crystal structure. SEM images, together with EDX element mapping, show that all elements are distributed uniformly in NGT ceramics. Moreover, the grain size of NGT ceramics decreases with increasing Nb and

Ga concentration. A giant dielectric permittivity of 7×10^4 with low loss ~0.02 is found in NGT10 ceramics. The weekly electrons can be localized by the trapping defects in designated lattice states, leading to generate defect-dipoles and excellent dielectric properties. In addition, the dielectric permittivity and loss of these ceramics are almost temperature, frequency and bias electric fields independent, which is critical for supercapacitors in electronics.

Acknowledgments

This work was supported by the National Nature Science Foundation of China-NSAF under Grant 51802182 and 51773168, Shaanxi Province Nova Program of Science and Technology (Grant No. 2018KJXX-081), and in part by Fundamental Research Funds for the Central University (xjh012019025).

References

1 S. Krohns, P. Lunkenheimer, S. Meissner, A. Reller, B. Gleich, A. Rathgeber, T. Gaugler, H. U. Buhl, D. C. Sinclair, A. Loidl, The route to resource-efficient novel materials, Nat. Mater. 10 (2011) 899−901.

2 C. C. Homes, T. Vogt, S. M. Shapiro, S. Wakimoto, A. P. Ramirez, Optical response of high-dielectric-constant perovskite-related oxide, Sci. 293 (2001) 673−676.

3 P. Lunkenheimer, S. Krohns, S. Riegg, S. G. Ebbinghaus, A. Reller, A. Loidl, Giant dielectric constants in transition-metal oxides, Eur. Phys. J. Spec. Top. 180 (2009) 61−89.

4 W. B. Hu, Y. Liu, R. L. Withers, T. J. Frankcombe, L. Noren, A. Snashall, M. Kitchin, P. Smith, B. Gong, H. Chen, J. Schiemer, F. Brink, J. Wong-Leung, Electron-pinned defect-dipoles for high-performance giant permittivity materials, Nat. Mater. 12 (2013) 821-826.

5 T. T. Fang, H. K. Shiau, Mechanism for developing the boundary barrier layers of $CaCu_3Ti_4O_{12}$, J. Am. Ceram. Soc. 87 (2004) 2072-2079.

6 J. B. Wu, C. W. Nan, Y. H. Lin, Y. Den, Giant dielectric permittivity observed in Li and Ti doped NiO, Phys. Rev. Lett. 89 (2002) 217601.

7 S. rohns, P. Lunkenheimer, C. Kant, A. V. Pronin, H. B. Brom, A. A. Nugroho, M. Diantoro, A. Loidl, Giant dielectric constant up to gigahertz at room temperature, Appl. Phys. Lett. 94 (2009) 122903.

8 C. Zhao, J. Wu, Effects of secondary phases on the high-performance giant permittivity in titanium dioxide ceramics, ACS Appl. Mater. Inter. 10 (2018) 3680-3688.

9 Z. Liu, C. Zhao, B. Wu, J. Wu, Reduced dielectric loss in new giant permittivity (Pr, Nb) TiO_2 ceramics by suppressing adverse effects of secondary phases, Phys. Chem. Chem. Phys. 20 (2018) 21814-21821.

10 Y. Q. Wu, X. Zhao, J. L. Zhang, W. B. Su J. Liu, Huge Low-Frequency Dielectric response of (Nb, In)-dopted TiO_2 ceramics, Appl. Phys. Lett. 107 (2015) 242904.

11 X. H. Wei, W. J. Jie, Z. B. Yang, F. G. Zheng, H. Z. Zeng, Y. Liu, J. H. Hao, Giant permittivity properties of Zn, Nb co-doped TiO_2 with different phase structures, J. Mater. Chem. C. 3 (2015) 11005−11010.

12 X. Zhao, P. Liu, Dielectric and electric relaxations induced by the complex defect clusters in (Yb+Nb) co-doped rutile TiO_2 ceramics, J. Am. Ceram. Soc. 100 (2017) 3505−3513.

13 Y. L. Song, X. J. Wang, X. Q. Zhang, X. D. Qi, Z. G. Liu, L. L. Zhang, Y. Zhang, Y. Wang, Y. Sui, B. Song, Giant dielectric permittivity in (Al + Nb) co-doped rutile SnO_2 ceramics with low loss at room temperature, Appl. Phys. Lett. 109 (2016) 142903.

14 J. L. Li, F. Li, C. Li, G. Yang, Z. Xu, S. J. Zhang, Evidence of grain boundary capacitance effect on the giant dielectric permittivity in (Nb+In) co-doped TiO_2 ceramics, Sci. Rep. 5 (2015) 8295.

15 J. L. Li, F. Li, Y. Y. Zhuang, L. Jin, L. H. Wang, X. Y. Wei, Z. Xu, S. J. Zhang, Microstructure and dielectric properties of (Nb+In) co-doped rutile TiO_2 Ceramics, J. Appl. Phys. 116 (2014) 074105.

16 X. J. Cheng, Z. W. Li, J. G. Wu, Giant permittivity in niobium and trivalent co-doped TiO_2 ceramics, J. Mater. Chem. A. 3 (2015) 5805−5810.

17 Z. Gai, Z. Cheng, X. Wang, L. Zhao, N. Yin, R. Abah, M. Zhao, F. Hong, Z. Yu, S. A. Dou, Giant Dielectric Constant of an Amorphous TiO_2:(Nb, In) Film with Low Loss Fabrication at Room Temperature, J. Mater. Chem. C. 2 (2014) 6790−6795.

18 W. Hu, K. Lau, Y. Liu, R. L. Withers, H. Chen, L. Fu, B. Gong, W. Hutchison, Giant dielectric permittivity in (Nb+Al) codoped rutile TiO_2 ceramics: compositional gradient and local structure, Chem. Mater. 27 (2015) 4934−4942.

19 K. Tsuji, H. Han, S. Guillemet-Fritsch, C.A. Randall, Dielectric relaxation and localized electron hopping in a giant dielectric (Nb, In)-doped TiO_2 rutile nanoceramics, Phys. Chem. Chem. Phys. 19 (2017) 8568.

20 X. G. Zhao, P. Liu, Y. C. Song, A. P. Zhang, X. M. Chen, J. P. Zhou, Origin of giant permittivity in $(In_{1/2}Nb_{1/2})TiO_2$ via broadband dielectric spectroscopy, Phys. Chem. Chem. Phys. 17 (2015) 23132.

21 T. Nachaithong, P. Kidkhunthod, P. Thongbai, S. Maensiri, Surface barrier layer effect in (In+ Nb) co-doped TiO_2 ceramics: an alternative route to design low dielectric loss, J. Am. Ceram. Soc. 100 (2017) 1452-1459.

22 Z. J. Wang, M. H. Cao, Q. Zhang, H. Hao, Z. H. Yao, Z. H. Wang, Z. Song, Y. M. Zhang, W. Hu, H.X. Liu, Dielectric relaxation in Zr doped SrTiO3 ceramics sintered in N2 with giant permittivity and low dielectric loss, J. Am. Ceram. Soc. 98 (2015) 476-482.

23 S. Yakovlev, C. Y. Yoo, S. Fang, H. J. M. Bouwmeester, Phase transformation and oxygen equilibration kinetics of pure and Zr-doped $Ba_{0.5}Sr_{0.5}Co_{0.8}Fe_{0.2}O_3$ perovskite oxide probed by electrical conductivity relaxation, Appl. Phys. Lett. 96 (2010) 254101.

24 S. Jesurani, S. Kanagesan, M. Hashim, I. Ismail, Dielectric properties of Zr doped $CaCu_3Ti_4O_{12}$ synthesized by sol-gel route, J. Alloys. Compd. 551 (2013) 456-462.

25 M. A. Subramanian, D. Li, N. Duan, B. A. Reisner, A. W. Sleight, High dielectric constant in $ACu_3Ti_4O_{12}$ and $ACu_3Ti_3FeO_{12}$ phases, J. Solid State Chem. 151 (2000) 323−325.

26 T. B. Adams, D. C. Sinclair, A. R. West, Giant barrier layer capacitance effects in $CaCu_3Ti_4O_{12}$ Ceramics, Adv. Mater. 14 (2002) 1321−1323.

27 Y. Song, X. Wang, Y. Sui, Z. Y. Liu, Y. Zhang, H. S. Zhan, B. Q. Song, Z. G. Liu, Z. Lv, L. Tao, J. K. Tang, Origin of giant dielectric permittivity of rutile $Ti_{0.9}In_{0.05}Nb_{0.05}O_2$: single crystal and polycrystalline, Sci. Rep. 6 (2016) 21478.

28 G. Liu, H. Q. Fan, J. Xu, Z. Y. Liu, Y. W. Zhao, Giant permittivity and impedance analysis of niobium and aluminum co-doped TiO_2 ceramics, RSC Adv. 6 (2016) 48708−48714.

29 P. Anithakumari, B. P. Mandal, S. Nigam, C. Majumder, M. Mohapatra, A. K. Tyagi, Experimental and theoretical investigation of the high dielectric permittivity of tantalum doped titania, New J. Chem. 41 (2017) 13067−13075.

30 W. Tuichai, S. Danwittayakul, P. Srepusharawoot, P. Thongbaia, S. Maensiri, Giant dielectric permittivity and electronic structure in (A^{3+}, Nb^{5+}) co-doped TiO_2 (A=Al, Ga and In), Ceram. Int. 43 (2017) S265−S269.

31 Z. W. Li, J. G.Wu, W. J.Wu, Composition dependence of giant permittivity in $(Sm_{0.5}Ta_{0.5})xTi_1{-}xO_2$ ceramics, J. Mater. Chem. C. 3 (2015) 9206−9216.

32 M. Y. Tse, M. K. Tsang, Y. T. Wong, Y. L. Chan, J. H. Hao, Simultaneous observation of up/down conversion photoluminescence and giant permittivity properties in (Er+Nb) co-doped TiO_2 materials, Appl. Phys. Lett. 109 (2016) 042903.

33 X. W. Wang, B. H. Zhang, L. H. Xu, X. E. Wang, Y. C. Hu, G. H. Shen, L. Y. Sun, Dielectric properties of Y and Nb co-doped TiO_2 ceramics, Sci. Rep. 7 (2017) 8517.

34 Z. W. Li, J. G. Wu, D. Q. Xiao, J. G. Zhu, W. J.Wu, Giant permittivity in titanium dioxide ceramics modified by tantalum and trivalent elements, Acta. Mater. 103 (2016) 243−251.

35 Y. C. Song, P. Liu, X. G. Zhao, B. C. Guo, X. L. Cui, Dielectric properties of $(Bi_{0.5}Nb_{0.5})_xTi_{1-x}O_2$ ceramics with giant permittivity, J. Alloys. Compd. 722 (2017) 676−682.

36 Y. Chao, X. H. Wei,J. H. Hao, Giant permittivity in TiO_2 co-doped by donor Nb and isovalent Zr, J. Am. Ceram. Soc. 101 (2018) 307–315.

37 M. Cancarevic, M. Zinkevich, F. Aldinger, Thermodynamic assessment of the PZT system, J. Ceram. Soc. Jpn. 114 (2006) 937-949.

38 W. Tuichai, P. Srepusharawoot, E. Swatsitang, S. Danwittayakuld, P. Thongbai, Giant dielectric permittivity and electronic structure in (Al+Sb) co-doped TiO_2 ceramics, Microelectron Eng. 146 (2015) 32-37.

39 H. Han, P. Dufour, S. Mhin, J. H. Ryu, C. Tenailleau, S. Guillemet-Fritsch, Quasimetrics giant permittivity in Nb and in co-doped rutile TiO_2 nanoceramics synthesized through an oxalate chemical-solution route combined with spark plasma sintering, Phys. Chem. Chem. Phys. 17 (2015) 16864-16875.

40 X. L. Cun, P. Liu, B. C. Guo, Y. C. Song, Stable giant permittivity and low loss in $(In_{0.5}Nb_{0.5})_{0.005}Ti_{0.995}O_2$ + x mol% $ZrTiO_4$ composite ceramics under DC bias voltage, Journal of Materials Science: Materials in Electronics 29 (2018) 18441–18448.